Apophyseal Ossification of the Iliac Crest in Forensic Age Estimation: Computed Tomography Standards for Modern Australian Subadults

Lottering, Nicolene; Alston-Knox, Clair L.; MacGregor, Donna M.; Izatt, Maree T.; Grant, Caroline A.; Adam, Clayton J.; Gregory, Laura S.

Published in:
Journal of Forensic Sciences

DOI:
10.1111/1556-4029.13285

Apophyseal Ossification of the Iliac Crest in Forensic Age Estimation: Computed Tomography Standards for Modern Australian Subadults*

Nicolene Lottering[1], *B.For.Sc, B.App.Sc (Hons), PhD*

Clair L. Alston-Knox[3], *B.Math (Hons), M.Sc, PhD*

Donna M. MacGREGOR[2], *B.Sc (Hons), M.Sc (For.Sc)*

Maree T. Izatt[4], *BPhty*

Caroline A. Grant[4], *B.Eng, M.Eng, PhD*

Clayton J. Adam[4], *B.Eng (Hons), PhD*

Laura S. Gregory[2], *B.Sc (Hons), PhD*

[1]Discipline of Anatomy and Pathology, School of Medicine, The University of Adelaide, Adelaide, South Australia, Australia, 5005.
[2]Skeletal Biology and Forensic Anthropology Research Laboratory, School of Biomedical Sciences, Faculty of Health, Queensland University of Technology, Brisbane, Queensland, Australia 4001.
[3]Social and Behavioural Research College, Griffith University, Mt Gravatt, Queensland, Australia 4122.
[4]Paediatric Spine Research Group, Institute of Health and Biomedical Innovation, Queensland University of Technology, and Mater Health Services, Brisbane, Queensland, Australia 4001.

*Presented at the 68th Annual Meeting of the American Academy of Forensic Sciences, February 22-27 2016, in Las Vegas, NV

Number of Pages: Text (19 pages); References (5 pages); Figure Legends (3 pages); Tables (9)/Figures (8)

Short Title: Ontogeny of the Iliac Crest Apophysis in Subadults

Corresponding Author:

Dr. Nicolene Lottering

Discipline of Anatomy and Pathology

School of Medicine, The University of Adelaide

Adelaide, South Australia, Australia 5005

Tel: +61 8 8138 5342 | Email: nicolene.lottering@adelaide.edu.au

Abstract

This study contrasts the ontogeny of the iliac crest apophysis using conventional radiography and multi-slice computed tomography (MSCT), providing probabilistic information for age estimation of modern Australian subadults. Retrospective abdomino-pelvic MSCT data acquired from 524 Australian individuals aged 7-25 years and surveillance radiographs of adolescent idiopathic scoliosis patients included in the Paediatric Spine Research Group progression study (n=531) were assessed. Ossification scoring of pseudo-radiographs and three-dimensional (3D) volume rendered reconstructions using Risser (1958) quantitative descriptors indicate discrepancies in age estimates, stage allocation and conflicting morphological progression. To mitigate visualization limitations associated with two-dimensional radiographs, we provide and validate a modified 3D-MSCT scoring-tier of ossification, demonstrating complete fusion between 17.3–19.2 and 17.1–20.1 years in males and females. Legal demarcation for *doli incapax* presumption and age of majority (18 years) can be achieved using probability estimates from a fitted cumulative probit model for apophyseal fusion using the recalibrated standards.

Keywords: Forensic Science; Forensic Anthropology; Subadult Age Estimation; Radiological Standards; Cross Sectional Studies; Iliac Crest Apophysis; Risser Score; Transition Analysis.

Introduction

Combined with clinical indicators including repeat height measurements, secondary sexual characteristics and the onset of menarche, the iliac crest has proven to be of considerable clinical value to estimate remaining growth potential and therefore the likelihood of pathological progression in patients with adolescent idiopathic scoliosis (AIS), influencing clinical intervention decisions such as the timing of bracing or surgery. In the mid-20th century, orthopaedic surgeon Joseph C. Risser developed a grading system for evaluating the iliac crest apophysis with the aim of providing additional information on the risk of progression of spinal deformity in individuals with scoliosis – the Risser sign (1). The apophysis of the iliac crest also provides possibilities for determining skeletal age due to its relatively late completion of maturation (2, 3). Wittschieber and colleagues (4) proposed the utility of the Risser sign for forensic age estimation in living individuals, particularly for the demarcation of the 14th year of life. However, the temporal pattern of iliac crest ossification proposed by Risser (1) has been contentious, with a meta-data analysis by Little and Sussman (5) suggesting that Risser's claim that ossification commences anterolaterally (termed as *capping*) from a single ossification center and fusion of the completed apophysis with the ala of the ilium commences posteromedially, cannot be substantiated. Furthermore, questions regarding the accuracy of the Risser sign in ossification assessment using plain radiographs have been raised with respect to 58% disagreement of Risser staging between posteroanterior and anteroposterior projections (6), radiographic foreshortening of the ilium and superimposition of the iliac crest on the sacroiliac joint posteromedially, and intrinsic individual variability in the iliac crest apophysis excursion and fusion (7, 8). Anomalous patterns of apophyseal ossification may introduce errors into Risser stage calculations, reflected by variable levels of inter-rater reliability (9-12).

From the standpoint of post-mortem examination, apophyseal union of the iliac crest opposed to ossification progression yields greater forensic significance, as the secondary centers of the ilium are rarely excavated due to their fragility within the archaeological context (13). Accordingly, Table 1 provides a summary of studies that have examined apophyseal union of the iliac crest for forensic age estimation. Due to antiquity of the reference samples/collections employed in the aforementioned studies, the age standards derived are problematic as they discount positive secular changes in height and maturation (14-16), evidenced through advanced timings of ossification in the current milieu (17-19). Furthermore, estimation of age in one population that is derived from a different group ignores knowledge of differential environments or genetic differences among groups, which causes differences in maturational rates and generates significant error in age estimations (20-25). Thus, it is acknowledged that skeletal growth and developmental data must be as contemporary and applicable to the target population as possible.

Recently, Lottering et al. (26) demonstrated the potential utility of the spheno-occipital synchondrosis for successful discrimination of the age of majority of modern Queensland, Australian individuals, which currently constitutes 17 years of age under the *Juvenile Justice Act 1992* (QLD)

(ss.5, 6 ("child")). The statutory minimum age of criminal responsibility in all Australian jurisdictions is ten years of age under the Commonwealth *Criminal Code Act 1995* (s7.1) and *Crimes Act 1914* (s.4M), while under The United Nations (1985) "Standard Minimum Rules for the Administration of Juvenile Justice" and *United Nations Convention on the Rights of the Child* (UNCRC), the imprisonment of a child in adult prisons is a breach of the rights stipulated under the UNCRC (27). A common law principle of *doli incapax* operates in all Australian jurisdictions and countries such as New Zealand, South Africa, Ireland and The United States of America to name a few, which constitutes a rebuttable presumption that a child aged under 14 years is unaware of the wrongfulness of their actions in a criminal sense.

The overarching aim of the present study is to document the temporal ossification of the iliac crest apophysis and provide up-to-date age standards for modern Australian subadults, using clinically acquired, cross-sectional MSCT data. Firstly, we aim to validate the assertion proposed by Wittschieber and colleagues (28) concerning the discrimination power of the Risser sign of demarcating the age of *doli incapax*, by recalibrating existing, antiquated standards for clinical assessment in a modern Australian population using conventional radiography. Since the Risser sign is routinely used in AIS examination, we provide standards for scoliosis patients and non-scoliosis subadults, and assess whether idiopathic scoliosis patients demonstrate divergent growth and development of the iliac crest apophysis. Circumventing radiographic limitations, a modified scoring-tier is presented for forensic age estimation based on the complete ontogenic sequence (appearance and fusion) of the iliac crest, which aims to provide up-to-date probabilistic information for post-mortem examination of modern Australian children using MSCT data, overcoming demographic composition and temporality biases.

Materials and methods

Paediatric Enterprise PACS, 'Trauma-screened' Queensland Dataset:

The sample comprised of de-identified retrospective abdomino-pelvic DICOM datasets acquired from 524 multi-ancestral individuals (females: 241, males: 283) aged 7-25 years, subject to multi-slice computed tomography (MSCT) scanning in the Departments of Medical Imaging at Queensland (Australian) Hospitals between 2007 and 2015. Thin-slice DICOM datasets with a maximum slice thickness of 1mm and overlap of 0.3mm were sourced from the Enterprise PACS database (D.W.), onsite at the Lady Cilento Children's Hospital (formerly the Royal Children's Hospital) and the Mater Health Services, South Brisbane, prior to anonymization in OsiriX® (Version 4.1 – 64 bit) (Visage Imaging GmbH, San Diego, USA). Since the Enterprise PACS database constitutes a central repository for all medical imaging datasets acquired from Queensland Health hospitals (North-Eastern Australia); 30.03% of scans were sourced from patients admitted to The Lady Cilento Children's Hospital/Royal Children's Hospital and Royal Brisbane Women's Hospital in Brisbane (CBD), 28.69% acquired from Gold Coast University Hospital (South East), 19.95% from

Central Queensland, Witsunday Coast and Wide Bay Burnett Hospitals (i.e. Mackay Base, Bundaberg, Rockhampton, Proserpine and Hervey Bay hospitals), and 21.07% from the Toowoomba Hospital (South West, Darling Downs). Biological parameters including the patient's date of birth, date of scan, institution/hospital name, sex and weight were embedded into the meta-data of each DICOM dataset, with chronological age and sex distribution of the sample depicted in Figure 1A. To be included in this study, scans had to include both the ischial tuberosity and iliac crest in the field of view. Exclusion parameters: individuals exhibiting signs of, or documented to have suffered from, metabolic or skeletal disorders that might influence normal growth and development i.e. osteogenesis imperfecta, skeletal dysplasia, Rickets, primary metastases, acute trauma pathology and previously documented abnormal bone age examinations. Since the majority of these individuals were referred for imaging by the emergency departments, this subsample will be denoted as "trauma-screened" individuals, for the purpose of this manuscript. These datasets constitute the latest addition of MSCT scans to "The Skeletal Biology and Forensic Anthropology Virtual Osteological Database" (29), housed at the Queensland University of Technology.

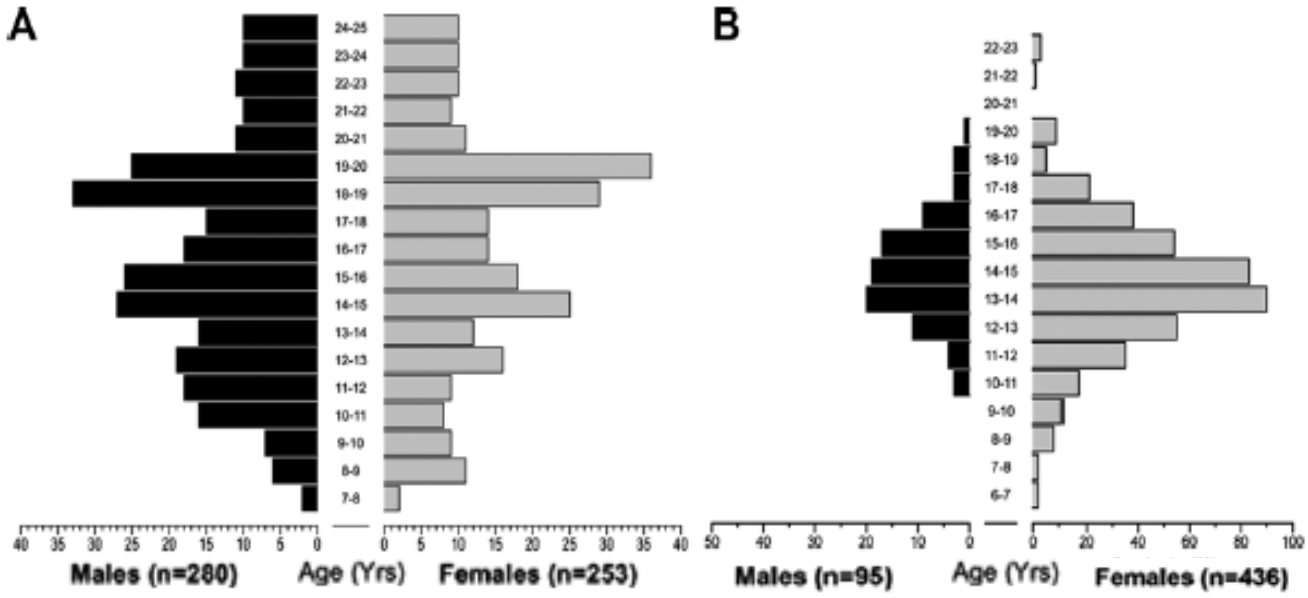

FIG. 1–*Age and sex distribution of the clinical sample of multi-ancestral subadults obtained from the Queensland Health Enterprise PACS database comprising Queensland, Australian individuals scanned between 2007 – 2015 (A) and Juvenile/Adolescent Idiopathic Scoliosis patients included in the Paediatric Spine Research Group Progression Study (1995 – 2007) (B). The frequency of male (black) and female (grey) individuals in each age cohort (years) are depicted.*

Idiopathic Scoliosis Dataset:

Analytic data were accessed from conventional scoliosis surveillance postero-anterior radiographs of the spine and pelvis from 531 patients (females: 436, males: 95) aged 6 – 23 years (distribution summarized in Fig. 1B) with juvenile or adolescent idiopathic scoliosis enrolled in a scoliosis progression risk study performed by the Paediatric Spine Research Group between 1995 and

2007. Growth and deformity parameters for each patient including Risser stage, Cobb Angle, standing height, weight and date of menarche, were documented by two highly experienced spinal orthopaedic surgeons and a highly experienced spinal orthotist and research physiotherapist. To assess remaining growth potential based on the developmental status of the apophyseal iliac crest ossification, the United States six-stage Risser sign grading system was utilized in the assessment of the left innominate. Prior to and during examination, radiographic assessment of the Risser Sign was performed blind to the age of the individuals. Patients with congenital scoliosis as well as scoliosis with an underlying neurological disorder, a syndrome or endocrinopathy were excluded from the progression study.

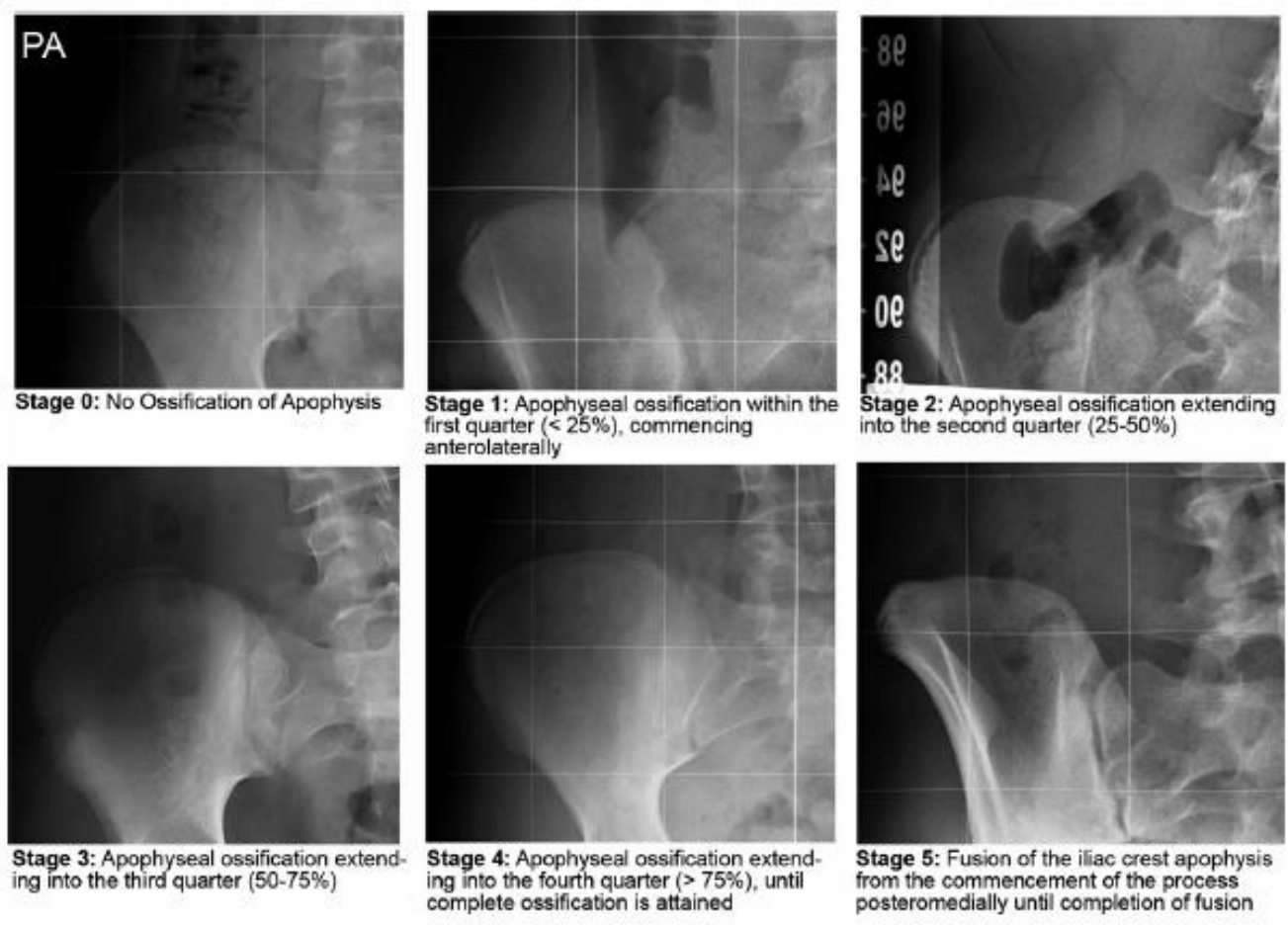

FIG. 2–*Risser Sign (1958): ossification stages of the iliac crest, with descriptions and examples based on posteroanterior, plain film radiographs, utilized as reference images in the Paediatric Spine Research Group Progression Study.*

Ossification Scoring

Two-dimensional images replicating the appearance of plain film radiographs were generated using thick-slab multi-planar reformatting volume averaging reconstructions of MSCT DICOM data, dubbed "pseudo-radiographs" in OsiriX (Version 4.1 – 64 bit) (Visage Imaging GmbH, San Diego, USA). This technique produces MSCT scout images, using a coronal reformat, resliced

with a thickness of 5mm slabs, to mimic the orientation and field of view of posteroanterior, standing radiographs employed in Risser staging for clinical assessment of growth potential (30). Based on the dissemination by Hatch and colleagues (30), we make the assumption that PR qualitative scores are comparable to those obtained from AP radiographs, based on visualization quality. In order to evaluate the developmental status of apophyseal iliac crest ossification, the Risser sign grading system, based on a six-stage system in which the apophysis is subdivided into quarters was employed (Fig. 2).

Consistent with post-processing protocols recommended by Lottering et al. (31)or morphological analyses of MSCT data, multi-planar reformatted (MPR) and volume-rendered reconstruction (VRR) models were generated in OsiriX® to visualise and subsequently score the degree of ossification of the iliac crest apophysis using 3D analysis. Apophyseal grading was initially conducted using the Risser sign scoring-tier and associated descriptions, to complement the approach for pseudo-radiograph assessment, however, preliminary examination revealed serious concerns regarding the application of Risser stages 1 – 3, as the apophyseal excursion did not proceed in the reported anterior to posterior linear pattern in our sample (1). Therefore, a modified seven-stage scoring tier, specific to 3D-MSCT was developed to reflect the ontogenic changes from apophyseal appearance to complete fusion. The new scoring-tier employed the quantitative descriptions (percentage ossified) published by Risser (3) for MSCT stages 0 – III and forensic convention of *commenced* (stage IV), *active* (stage V) and *complete union* (stage VI). It should be noted that the modified MSCT scoring-tier originally comprised eight stages (scored for all individuals); exploratory data analysis demonstrated significant overlap between Risser stages 1 and 2, prompting these stages to be pooled into MSCT stage I. Table 2 summarises the features used to score the maturation of the apophysis in MSCT using the ordinal seven-stage system and in combination with the illustrations provided in Figure 3, provides a quick reference chart that can be utilized in the laboratory or in clinical medical imaging examinations.

Due to the concerns discussed in Lottering et al. (31) pertaining to partial volume effects and pseudo-fusion of volume rendered reconstructions associated with threshold-based algorithms, which lack the ability to successfully discriminate between materials with similar density properties, an orthogonal plane MPR technique is preferred for assessment of fusion status. Orthogonal plane MPR provides three perpendicular planes displayed simultaneously with graphical cues indicating their relative orientations and intersections, which can be moved within the 3D image volume to provide a cross sectional view at any desired location along the adjusted principal component axes. Radiographic appearance of the bone tissue in the DICOM stack allows for an intricate and more accurate assessment of bony bridging and cortical bone interruptions; the latter obscured in volume rendered reconstructions.

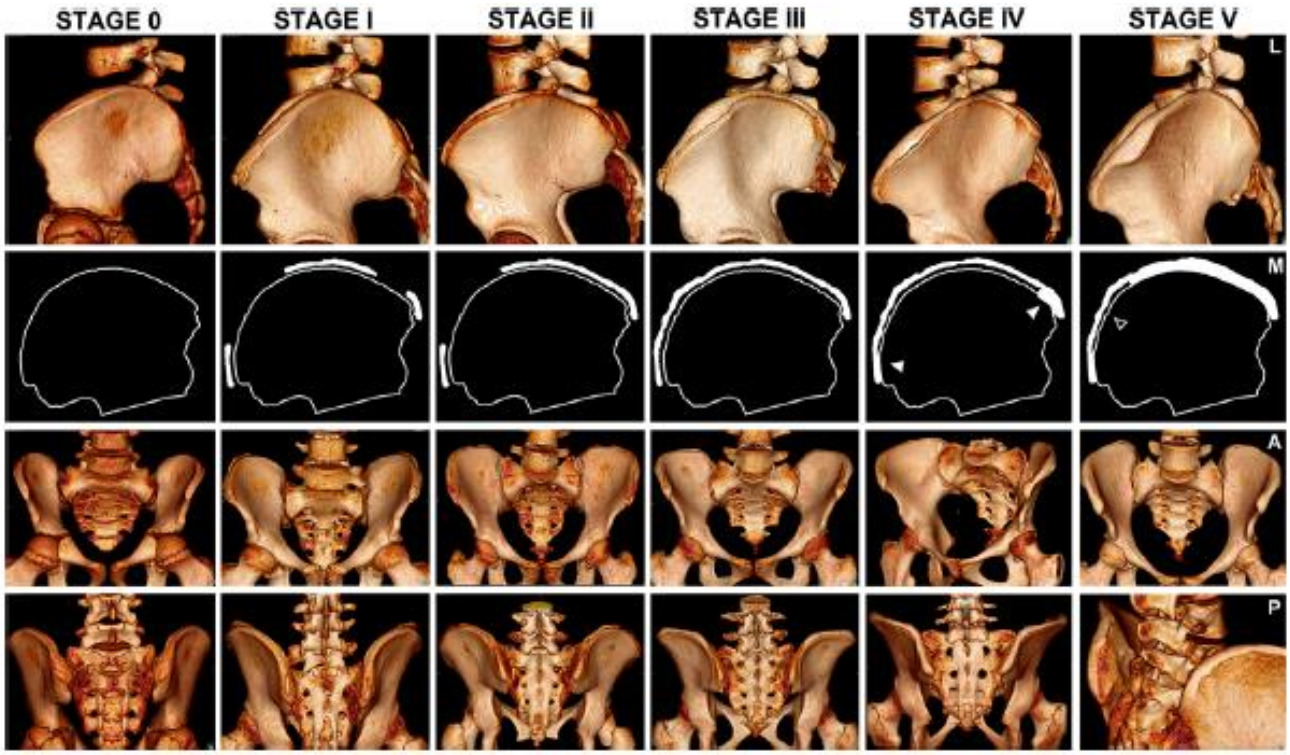

FIG. 3–*Stages of Apophyseal ontogeny (appearance and fusion) based on a modified seven-stage system using 3D-MSCT volume rendered reconstructions to complement text descriptions provided in Table 2. Osseous silhouette drawings of the medial ilium (thin contour) and secondary ossification center (white, thick lines) depict the development of the iliac crest apophysis in stages 0 – III and epiphyseal fusion in stages IV – V. Regions denoting 'commenced fusion' are highlighted by white, filled arrows; the postero-medial aspect of the ilium deficient of fusion in stage V (active/advanced fusion) is illustrated by the clear arrow. NOTE: Stage VI (complete union) is not represented. Perspectives: left lateral (A), left medial (M), anterior/oblique (A) and posterior/oblique (P).*

Gantry tilt helical MSCT frequently constitutes part of the pediatric scan protocol in Children's hospitals, by shifting the Y-axis direction by tilting the gantry of the scanner, in an attempt to avoid radiation exposed to external genitalia and lymphatic organs. Failure to compensate for the direction and angle of the tilt results in distortion of the DICOM data and consequently inaccurate model reconstruction; correction for the tilt (+/- 30 degrees) was conducted using the OsiriX® plugin. For consistency, DICOM data was viewed with a bone algorithm at a window level of 350HU and width of 2700HU, consistent with standardized protocols employed by our laboratory (26, 31). It should be acknowledged that the utility of MPR requires substantial anatomical imaging interpretation and without a volume reconstruction, users are required to mentally transform 2D images to form a 3D impression of skeletal structures, which may introduce a certain degree of error. Accordingly, all scores using the modified MSCT system were verified on VRR models generated with the inbuilt OsiriX® bone algorithm window parameters, serving as a three-dimensional skeletal replica of the innominate.

Observer Error

To assess the reliability attributed to the Risser staging system, repeat assessment of thirty randomly selected abdominopelvic pseudo-radiographs was conducted by five independent observers with varied anthropological, orthopedic and/or medical imaging experience, on two different occasions (minimum of 24 hours between reexamination). Under identical conditions, MPR/VRR assessment of the same scans was conducted to quantify inter-rater reliability (IRR) and evaluate the utility of the proposed MSCT scoring descriptions (Table 2) and illustrations (Fig. 3). To evaluate method repeatability, the first author conducted repeated examination on three different occasions with a minimum of 24 hours between re-examination, for both scoring systems. As a measure of reliability, the intraclass correlation coefficient (ICC), specifically a two way random, average-measures model, with consistency type 95% tolerance interval was calculated in SPSS, version 22 (2013; IBM Corporation, Armonk, NY) measuring the proportion of variance that is attributable to object measurements (32).

Cumulative Probit Regression

Consistent with the methodological approach utilized in our previous publications (26, 31, 33), the data were analysed as a cumulative probit model. The cumulative probit regression, the details of which are expounded in Konigsberg (34), has proven an efficient tool for age estimation based on ordinal developmental scores. A Bayesian analysis using a latent trait structure has been utilized to explore the structure of this data. The aim of the latent variable approach is to estimate the underlying continuous trait that is hidden within the necessarily discretised measured developmental scores. The estimates of the latent trait were used to better model the parameters of the cumulative probit model.
The ordered probit model can be represented as:

$$\mathrm{P}(y \leq \mathrm{j}) = \Phi\,(\gamma_j - \beta_{i*}\,x),$$

where j represents the stage of development, Φ represents the standard normal cumulative density function, γ_{j} is the intercept for the cumulative probability of being in stage j, x is the design matrix containing terms for age, health status and sex, along with interaction between these terms. As such, each β_{i*} is the estimated effect of health status, age and sex effects, and these can be tested for significant differences in response ($P < 0.05$). When the appropriate fixed effects are determined, the transition age was calculated as the point estimate of age at which it is most likely that group membership changes, specifically:

$$\text{Age at Transition} = {}^{\gamma_j}/_{\beta_{i*}}$$

In terms of the Markov Chain Monte Carlo (MCMC) scheme, vague priors were employed to model the transition of individuals from one developmental stage to another in an ordered sequence. Specifically, an ordered Probit Regression model on age, with sex and health status (for

Risser examination only) was fit using MCMC estimation with the "MCMCoprobit" function from the "MCMCpack" library (35) in "R" (http://www.r_project.org). This function utilizes a generalized linear model involving an intercept and regression slope, which is converted to the mean and standard deviation of transition age. Parameter estimation of fixed effects β and cutpoints γ is conducted using the algorithm proposed by Cowles (36) in which a latent variable approach simulates an additional continuous parameter based on the response (age indicators) and the current estimates of the fixed effects and cutpoints with the Gibbs sampler. In this framework, the use of the latent variable leads to simple MCMC updates of the posterior distributions for β and γ as Normal and Uniform variates (see algorithm 1.0 for 3-step Gibbs Sampler).

Algorithm 1.0 - Gibbs sampler for estimating Latent trait cumulative probit model
Iterate until convergence

1. For each subject in the data set, simulate a latent variable, y^*, from a standard Normal distribution;
   $y^* \sim N(\beta x, 1)$

2. Using the simulated latent variables, Y^*, update estimates of the fixed effects parameters, β from their posterior distribution;
   $\beta \mid X, Y^* = N((X^T X)^{-1} X^T Y^*, (X^T X)^{-1})$

3. Using the current estimates of y*, β and $\gamma_{k>j}$, update estimates of each cutpoint, γ_j;
   $(\gamma_j \mid Y^*, \gamma_{j-1}, \gamma_{j+1})$
   $= \boldsymbol{U}\,[(\max(\max\{y^*: y_i = j\}, \gamma_{j-1})),$
   $\min(\min\{y^*: y_i = j+1\}, \gamma_{j+1})].$

To complement the transition analysis, an extension to the model was performed to determine the posterior distribution of age of the Queensland population across each developmental stage. A Bayesian statistical approach was utilized to estimate the posterior distribution of age for each stage. The term 'posterior' defines the distribution of likely ages of individuals in the population that are generally associated with each category; the distribution of age defined using the proportional relationship:

$$p(\text{age} \mid c_j) \propto p(c_j \mid \text{age})\, p(\text{age})$$

where $p(c_j \mid \text{age})$ is the likelihood (sampling distribution) of being in category c_j given the individual's age, which is obtained from the cumulative probit modeling of the transition analysis. p(age) is the prior distribution of age; as adolescents constituted our target demographic, the prior distribution of age was assigned as a Uniform (6,25) prior (34, 37), due to a lack of skeletal reference material available for the Australian population. Under this scheme, the posterior distributions of age are calculated using a simulation process within the Gibbs sampler. The simulations are based on the following: At each iteration of the MCMC sampler,

1. Simulate 1000 new variates as W* ~ Uniform(6,25),
2. Based on the current estimates of γ and β, assign each w* to a category, c_j.

The output of these simulations is a sample drawn from the posterior distribution of age given development category, *p*(age|stage). The mean age of the posterior distribution, along with the standard deviation and credible intervals can be calculated from this sample (30). In this case, the α% credible interval is defined as the age range of the posterior sample i.e. exclusion of the top and bottom α/2.5% of sampled values for derivation of a 95% interval. Credible intervals ranging from 68% (±1SD) to 90% probabilities were also calculated. Since the study design did not include individuals under the age of 7 years, or over 25 years, age ranges are expressed as the oldest and youngest probable ages for the first and last stages, using one-tailed probabilities. Posterior probability tables of age for a given stage of union were constructed to provide a comprehensive insight into the age variation in development of the iliac crest, which can be used for age estimation of the subadult skeleton in the laboratory or field. It should be acknowledged that due to the cross-sectional design of this study, inferences of growth can only be made with respect to a significant number of morphological snap shots at successive chronological ages. Nonetheless, a cross-sectional approach is recommended for age estimation efforts as it offers a random sample of the population, thus the variability in development is far greater in comparison to a sample of the same children over time and avoids data heaping inherent with longitudinal designs (38, 39).

Results

Risser Sign Grading – Developmental Deviation

Inter-rater reliability (IRR) quantified using a two-way random, absolute-agreement ICC model, indicated 'excellent agreement' between five independent investigators, comprising of forensic anthropologists, spinal orthotists and biomedical engineers. The average-measures ICC comprises of 0.863 (95% CI: 0.73-0.93); while intra-observer analysis indicates approximately 7% discrepancy in absolute agreement with an ICC of 0.933 (95% CI: 0.88-0.97).

Estimates of age-at-transition for Queensland idiopathic scoliosis individuals are congruent with 'trauma screened' patients admitted to Queensland Children's Hospitals; the probit regression demonstrating no significant effects for health status ($P > 0.05$). Accordingly, scoliosis and trauma screened individuals were pooled and a cumulative probit model refit to collective Queensland data, with effects of age and sex. Irrespective of Risser stage, sex effects were significant ($P < 0.05$), demonstrating that apophyseal development of Queensland females is significantly more advanced (approximately 12 months earlier than males). For example, Queensland females transition between stages 0 and 1 (appearance of apophysis) at 12.89 ± 0.10 years, in contrast to males at 14.17 ± 0.11 years (Table 3). Figure 4 illustrates the sample data distribution and transition ages provide in Table 3, using the cumulative probit model, for Risser stage classification. Membership in stages 0-4 is generally restricted to ages 14 – 16 years, with a small number of 13 and 17 year olds represented. The distribution plot indicates that ages 14 to 16 years demonstrate the greatest ambiguity, with an almost

even membership probability across all Risser stages. This restricted age range in combination with the posterior distribution for the cutpoints of the probit model (Algorithm 1.0 – step 3) which uses estimation based on a narrow ordering, leads to overlapping credible intervals for the posterior distribution of age (Table 4).

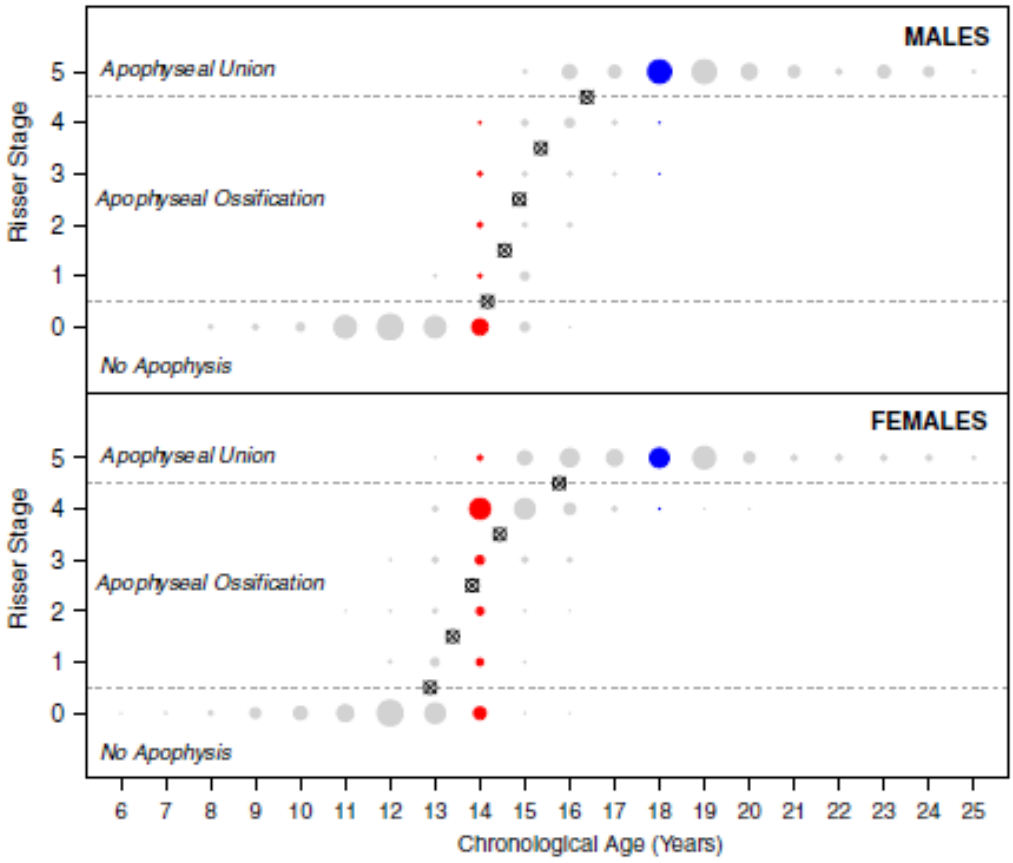

FIG. 4–*Distribution plot of individuals classified by age (years) and sex for Risser stage membership, to which the cumulative probit model was fit for Queensland males (top) and females (bottom). Dot size indicates the magnitude of the number of subjects for each age and stage. The open circles (with crosses) indicate the point estimation for the transition between stages as estimated by the cumulative probit model. Samples relating to the legal demarcation ages of 14 and 18 years are depicted in red and blue (online version).*

In accordance with Commonwealth legislative ages, Table 5 provides probability estimates of belonging to each Risser stage for ages 14 and 18 years based on the fitted cumulative probit model. It is evident that a 14-year-old female has a relatively equal probability of being classified into stages 0 to 3, and 27.0 – 36.8% probability of stage 4 assignment. For Queensland males, the 14 years demarcation cannot be confidently determined based on the 95% CI for Risser stage 1-3, with probabilities ranging from 9.9 – 10.4%; however if an individual presents with morphological indicators coherent with stage 4 (the apophysis had attained lengthwise dimensions; apophyseal cartilage not ossified), it is 89-95% probable that he is older than 14 years.

Risser scoring of pseudo-radiographs (PR) and 3D-MSCT of the same individuals that constitute the trauma-screened sample using the Risser (1) quantitative descriptors i.e. stage 1: ≤ 25%

apophysis ossified, indicates discrepancies in stage allocation. For methodological comparison, the original scores of the initial eight-stage MSCT tier, where stage I was subdivided based on the original Risser 1 (≤ 25%) and 2 (25-50%) quantitative descriptors, were referred to. The high-low plot, represented in Figure 5, quantifies the directionality in Risser stage deviation (bias), scored on both modalities for the same individuals. Individuals classified into Risser stages 0 – 4 on PR constitute the baseline; comparative scoring on VRR indicates an underestimation of stage by at least one stage or more using PR. Specifically, the appearance of the anterior apophyseal center is delayed by one or more stages using PR, for 100% of individuals assigned a score of Risser 1 on VRR models (n=21). Queensland individuals classified into Risser stage 1 on PR, present with the morphology of Risser stage 2 (apophyseal length exceeds 25% of the length of the curvilinear superior border of the ala of the ilium) in 37.5% of cases, when scored on VRR. The commencement of fusion to the ala of the ilium is detected earlier in 3D-MSCT relative to conventional radiography. Risser stage 5 was assigned to *both* PR and VRR representations of the same individual in 84.8% of cases, with PR only overestimating age, suggesting pseudo-fusion with the ilium in 15.2% of individuals.

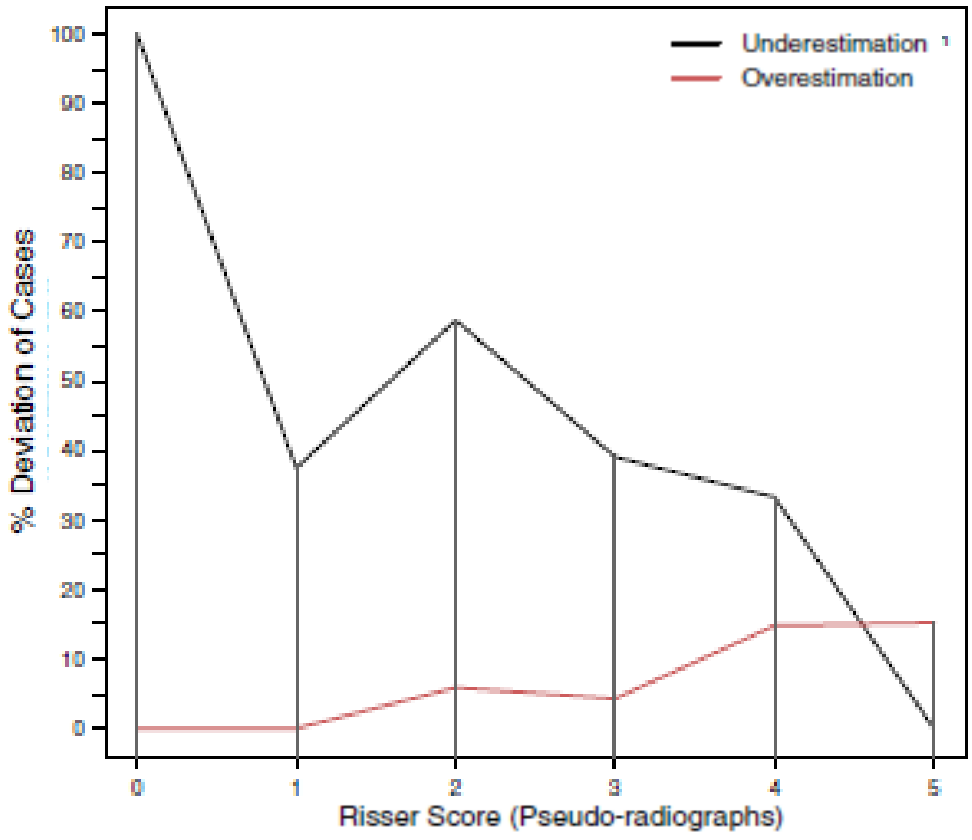

FIG. 5–*Directionality of Error (Bias) in Risser Stage Classification for Queensland Individuals, scored on thick-slab pseudo-radiographs and 3D-MSCT volume rendered reconstruction models. For individuals classified into respective Risser stages using pseudo-radiographs (x-axis), the percentage of cases underestimated (black) and overestimated (red) by at least one stage in comparison to 3D-MSCT scores is represented. The percentage of cases for each stage totals 100%; data not shown is indicative of equal scores assigned on both PR and 3D-MSCT.*

Ontogeny of the Iliac Crest Apophysis using MSCT

Precision testing of the modified 3D-MSCT scoring-tier denotes minimal measurement error among five independent investigators, confirming the suitability and reliability of the morphological descriptors (Table 2) and accompanying illustrations (Figure 3) for ossification scoring of the iliac crest apophysis. Specifically, IRR constitutes an average-measures ICC of 0.993 (95%CI: 0.98-0.99), while intra-observer analysis indicates consistent re-examination with less than 1% discrepancy between score assignment (ICC: 0.994; 95%CI: 0.98-0.99).

Morphological observation using 3D-MSCT demonstrates that the anterior apophysis of the iliac crest develops from two secondary ossification centers, segregated based on its location at the anterior superior iliac spine (ASIS) and/or adjacent to the body of the ilium at the site of the iliac tubercle (antero-lateral flare of the ilium) (Fig. 3; column1). In 69.9% of Queensland individuals, the iliac tubercle center will be the first to commence ossification. Generally, the posterior apophysis superior to the PSIS appears after the anterior apophysis in 66.8% of the sample. As demonstrated in stage I (Fig. 3), the three centers constitute separate entities, with distinct cartilaginous gaps or *skip ossification* between them. In stage II, union of the ASIS and tubercle ossification centers of the anterior apophysis has commenced, with the lateral margins continuous with each other, while appositional growth of the posterior apophyseal center is minimal in comparison (less than half its maximum anteroposterior dimension). Transition between stages II/III (complete appositional growth) occurs significantly earlier in females at 14.90 ± 0.17 years compared to males at 15.75 ± 0.13 years ($P < 0.05$) (Table 6; Fig. 6); apophyseal growth is complete between the ages of 11.61 and 16.84 years in females and 13.05 and 16.89 years in males, demonstrating substantial variability. Estimates for transition stages characterised by *degree of fusion* to the ilium (III-IV to V-VI), demonstrate greater discriminant power with less overlap of the density distributions (Table 6; Fig.6), than stages associated with appositional growth patterns. Ossification of the apophyseal cartilage commences on the anteromedial aspect of the ala of the ilium, significantly earlier at 12.62 years of age in Queensland females, in contrast to 13.82 years in males ($P < 0.05$) based on the lower extremity of the 95% credible intervals (Table 7). Fusion of the postero-medial surface of the iliac crest, superior to the iliac tuberosity and adjacent to the sacro-iliac articulation, which constitutes the insertion of the erector spinae muscle group is significantly delayed (Fig. 3; stage V, posterior). Fusion of the iliac crest is complete by 19.22 years (oldest probable age of Stage V) in males, approximately 11 months earlier than females, which exhibit complete fusion prior to 20.07 years (95% CI; Table 7).

Forensic Standards for Age Estimation

Table 8 illustrates the female results of a validation study conducted on a random, independent sample of 40 Queensland individuals (n=20/sex), obtained from the *Skeletal Biology and Forensic Anthropology Research Osteological Database*, not included in the model construction. Error

was quantified using measures of inaccuracy ((Σ|estimated age - actual age|)/*n*) and bias ((Σ(estimated age - actual age)/*n*), where *n* is the number of samples, estimated age is the posterior mean age (or oldest/youngest probable age if assigned to stages 0 or VI) of the classified stage and actual age refers to chronological age. The Bayesian posterior probabilities presented in Table 7 demonstrate correct classification of 67.5% and 80% of the validation sample based on the 90% and 95% CIs pooled for males and females, respectively. Collectively, the 3D-MSCT scoring-tier demonstrated a tendency to underestimate age with an inaccuracy of 1.75 ± 0.97 years. We note that the "worst" estimated ages are from individuals that appear exceedingly immature or mature for their age, representing developmental outliers in the population. For example, the subject of chronological age 16.7 years of age, classified as a stage I demonstrates significantly delayed development, as results from the cumulative probit suggest that it is most probable that he/she should be assigned to stage IV. Figure 7 verifies the irregular nature of this estimate as the probability of this subject being a stage I is less than 10% and accordingly is not represented on the graph.

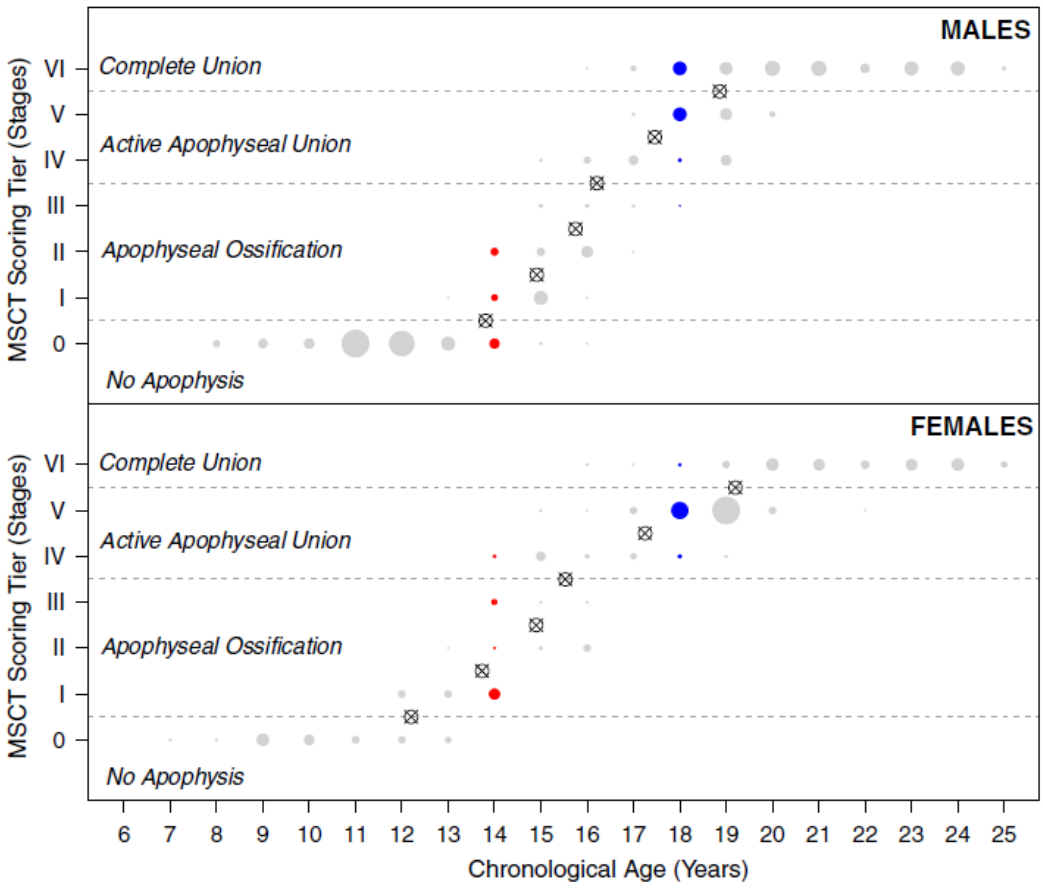

FIG. 6–*Distribution plot of data classified using the new 3D-MSCT scoring tier categorized by chronological age and sex. The magnitude of the dots represents the sample size for each age and stage category. The open circles (with crosses) represent the point estimates of transitions between consecutive stages based on the cumulative probit model for Queensland males (top) and females (bottom). Samples relevant to Commonwealth legal demarcation ages 14 and 18 years are illustrated in red and blue (online version), with probabilistic information provided in Table 9.*

Accordingly, for derivation of an age estimate in Australian casework using this skeletal site, Figure 7 may be helpful, depicting probabilistic estimation of MSCT stage given chronological age, *p*(stage| age), with only estimates greater than 10% shown. We suggest a systematic approach using age estimates based on ≥ 90% probabilities, and if no matches are yielded in the missing persons database, estimates consistent with the 75% and 50% probabilities may be consulted. If 90% probabilities cannot be calculated due to small sample sizes i.e. stages I – V, the highest weighted probability should be consulted. For example, if a suspected Queensland male presents with morphology consistent with stage 0, there is greater than 90% certainty that he is ≤ 12 years of age. Accordingly, there is a 75-89% probability that the individual may be 13 years of age, but only a 10-24% probability he may be as old as 15 years. Caution should be applied for age estimation using stages I – IV, which yield probabilities less than 50%. Complete fusion of the iliac crest, calculated with reference to the oldest probable age for stage V and youngest probable age for stage VI, occurs between 17.26 and 19.22 years in Queensland males, and 17.07 and 20.07 years in females (Table 7). Figure 7 corroborates these ranges, demonstrating that it is most likely that an individual classified in stage V is 18 years old, independent of sex; there is ≤ 24% likelihood that a 20-year-old male individual is assigned to stage V, relative to ≥ 75% probability of exhibiting complete fusion of the apophysis (stage VI).

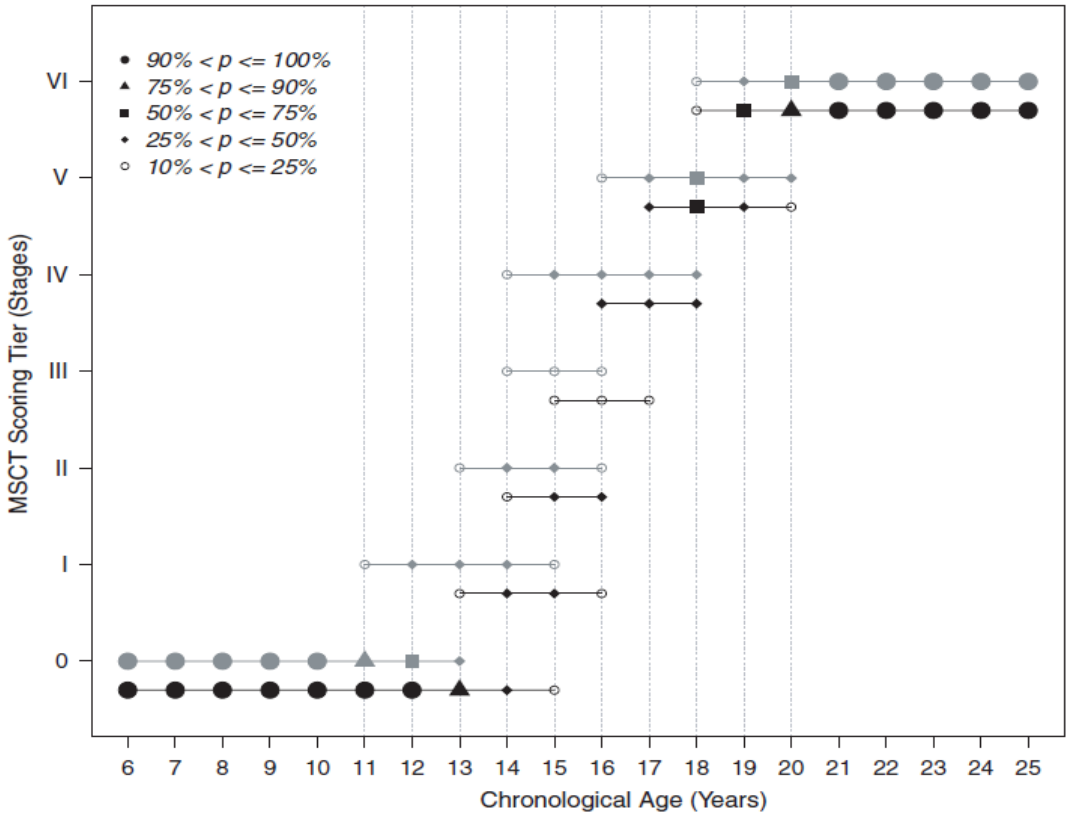

FIG. 7–*Weighted Dot Plot illustrating the probability of classification into the 3D-MSCT Scoring tier given chronological age, p(Stage|Age), for Queensland males (black symbols) and females (gray symbols). Probability estimates range from 10% (open circles) to 90+% (filled circles), based on 1500 thinned MCMC iterations. Probabilistic data can be utilized to derive an age range, at a given distribution level.*

Probability estimates of being classified into a particular maturation stage, given the Commonwealth legal demarcation ages (Table 9 and Fig. 7) based on the fitted cumulative probit model, demonstrate that the 18 year threshold can be estimated beyond reasonable doubt based on apophyseal union (stage IV- VI) for males (96.86%) and females (96.96%). Fig.7 illustrates the distribution of stage classification, weighted for probability estimates provided in Table 9, and demonstrates substantial variation in skeletal development between the ages of 14 – 17 years in males and 14 – 16 years in females. For the 14-year demarcation, it is 82.87% likely that Queensland males will be classified into stages 0/I in contrast to 66.31% probability of female classification into stages I/II. However, there is also a 7.1 – 18.5% probability that a 14-year-old female may present with morphology consistent with stages III and IV in the Queensland sample. Therefore, the 14-year demarcation cannot be confidently determined based on apophyseal ossification.

Discussion

Examination of the Risser Sign for Age Estimation

The current study recalibrates Risser age standards for an Australian sub-population, using a cumulative probit model to (i) calculate credible intervals ranging from 68% to 95% (Table 4) (ii) and provide probability estimates of chronological age given Risser stage; an approach less sensitive to developmental outliers and age mimicry. The posterior mean ages presented for Queensland children in Table 4 for stages 1 to 4 are younger than those reported by Wittschieber et al. (28), who used radiographs obtained from the Institute of Clinical Radiology of Munster University Hospital (2008-2010), such that the apophysis appears approximately four years earlier in Queensland females. Interestingly though, the onset of fusion (stage 5) commencing at 14.4 years in females and 15.3 years in males, is similar to the timings reported for German individuals (14.2 and 15.0 years, respectively) (28). Without a direct inter-population comparison, it is difficult to ascertain if this deviation is attributed to demographic bias or differences in statistical methodology and sample age distributions. Contrary to the proclamation by Wittschieber et al. (28), significant overlap in stage classification for Risser 1 – 4 between ages 13 – 16 years is evident, suggesting that apophyseal ossification is not an accurate indicator for subadult age estimation. Posterior distributions of age demonstrate that the apophysis is unfused under the age of 17.0 years, irrespective of sex (oldest probable age of stage 4); the onset of epiphyseal union (Risser stage 5), detected using conventional radiographs, may be a more promising indicator for demarcating the legal age of majority in Queensland under the *Juvenile Justice Act 1992* (QLD) (ss.5, 6 ("child")).

Conventional Radiography Limitations

The results of this study provide an overdue, cautionary note on the implications of routinely utilized imaging modalities such as plain film radiography for the evaluation of ossification status. In order to assess the accuracy of the Risser sign for age estimation using plain film radiography, it was necessary to compare the results obtained using posteroanterior PRs with MSCT volume-rendered reconstructions (VRR), that exhibit greater sensitivity in detection and morphological assessment of low-density woven bone tissue that constitutes recently formed ossification sites based on the extended range of the Hounsfield scale. To the best of our knowledge, this study constitutes the first to generate thick-slab coronal MPR volume averaging reconstructions (resliced thickness of 5mm) or PRs of 3D-MSCT DICOM data for paleodemographic research. Familiarity with such reconstruction techniques may enable forensic practitioners without MSCT scanners to create pseudoradiographs from antemortem MSCT data, for comparison with post-mortem conventional radiographs to facilitate personal identification, as discussed by Hatch et al. (30). 3D-MSCT provides superior detail of the mineralization patterns pertaining to the immature woven bone structure than conventional radiography. For example, Figure 8 illustrates the visualization discrepancy between staging based on the two modalities, with VRR demonstrating complete appositional growth of the apophysis and commenced fusion superolateral to the posterior superior iliac spine. The maximum intensity projection in Figure 8B illustrates a narrowed excursion on the superolateral aspect, which does not extend to the sacroiliac joint, which would be consistent with Risser stage 2 or 3. On the thick-slab PR, this region of interest is obscured (Fig. 8A) by radiolucent gas in the colon; the white arrow depicting a region where “pseudo-fusion” may be inaccurately inferred.

Risser (3) ascertains that maturation of the ilium manifests on pelvic radiographs, as progressive ossification of the apophysis, commencing at the anterior superior iliac spine (ASIS) and extending posteromedially toward the posterior superior iliac spine (PSIS). In contrast, macroscopic anthropological studies suggest that ontogeny of the iliac crest apophysis is variable and heterogeneous (37). Scheuer and Black (37) state that the iliac crest apophysis forms as two separate ossification centers, prior to uniting at the middle of the crest, posterior to the most superior point. 3D-MSCT in this study corroborates the latter assertion and provides a detailed insight into the appearance of ossification in the anterior apophysis from two segregated centers as well as the posterior apophysis. It is evident that the complex curvature of the ilium is not accurately represented in a single AP radiograph. Kotwicki (40) suggests that assessment of iliac apophysis excursion made exclusively using this projection misses 30% of the length of the excursion due to the foreshortening of the oblique iliac crest curvature and superimposition by the sacrum. The sagittal orientation of the posterior apophysis, located posterior to the sacroiliac junction, is not accounted for in the Risser

grading system or reported in radiographic studies, with the exception of those employing additional lateral projections.

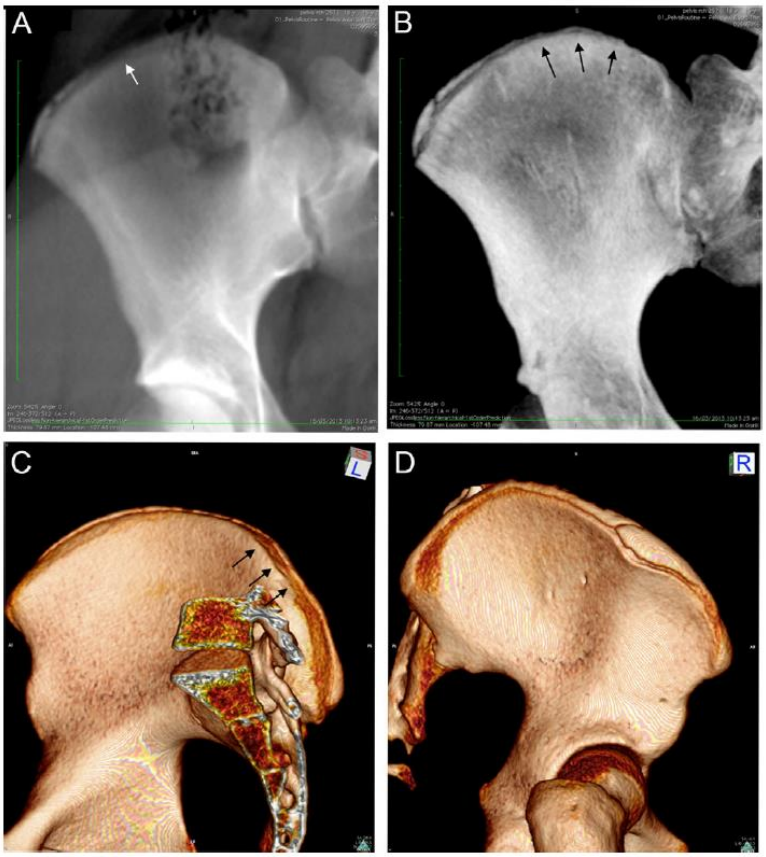

FIG. 8–*Example of Queensland Female (15 years), classified as Stage IV of the 3D-MSCT scoring system. Complete anteroposterior excursion of the iliac crest apophysis, compared to the maximum lengthwise dimension of the iliac bone from ASIS to PSIS, with partial fusion between the anterior/posterior apophyseal centers to form the iliac tubercle (D). Despite fusion commencing on the posterolateral aspect of the ilium, lateral to the PSIS, appositional growth of the posterior apophyseal center is incomplete, failing to extend to the medial surface of the iliac tubersosity (C). On a coronal pseudo-radiograph (MIP reformat; B), the apophysis is not visible (black arrows). Based on a mean reslice of 5mm increments (A), consistent with conventional radiography, the lateral transcendence of the apophysis presents as "pseudo-fused" (white arrow), while gas in the ascending colon partially obscures the field of view. Investigators not familiar with the three-dimensional ontogeny of the crest apophyseal fusion may confuse the coronal radiograph as stage II (greater than 50% of apophyseal ossification, with a large bone deficiency between the anterior and posterior centers, posterior to the most superior point of the iliac bone).*

Our findings demonstrate discrepancy in scoring between two-dimensional images i.e. plain film radiographs and/or PRs, and 3D-MSCT VRR models. PRs generally underestimated age by at least one Risser stage due to delayed detection of the iliac crest apophysis using a two-dimensional format (Fig. 5). Accordingly, comparisons of our MSCT results to the appearance of the apophysis reported in conventional radiographic studies such as that by Jit and Singh (41) and Garn et al. (42) are advised against. Obstruction of the field of view of the posterior aspect and complete excursion of the iliac crest is a major concern for scoring skeletal progression using PR in isolation, particularly for age estimation of unknown skeletal remains. Our search of the open-source Query

Patricia 4.1 radiographic database (39), performed for AP pelvic radiographs (ilium in the field of view) of white American individuals aged 8 – 20 years, demonstrated that only 22% (n = 72 / 326) of films were of appropriate quality for ossification scoring of the iliac crest apophysis. Copious amounts of gas and faecal material in the colon were evident in the majority of films, reducing visibility of the iliac crest. Since the Patricia 4.1 database was assembled from post-mortem radiographs, it can be assumed that the study samples reflect various stages of decomposition, i.e. bloating due to an increased bacterial and microbial activity and subsequent release of gaseous biproducts of cellular digestion, aggravating the issue of superimposition due to increased radiolucency in the large intestine. Consistent with autopsy protocols in most Australian mortuaries, where post-mortem MSCT scanning of skeletal remains is standard practice, we recommend the utility of the 3D-MSCT-specific standards for the estimation of age using the iliac crest apophysis, to reduce error attributed to scan quality and spatial orientation in conventional radiographs. Threshold-based image segmentation techniques for MSCT thin-slice data also alleviate such obstructions to the field of view by selectively removing voxels with material density properties consistent with soft tissue structures, fluids and air. For institutions without access to a MSCT scanner, we advocate maceration followed by scoring of ossification status on dry bone; with age estimates derived using the proposed 3D-MSCT standards (Table 7). We recommend that age estimates derived from conventional radiographs be approached with extreme caution.

Contributions to Age Estimation: 3D-MSCT Standards

It should be disclosed that although our data acquisition is specific to MSCT data, we do not advocate prospective MSCT scanning of living children for bone age examination. Instead, the significance of this study is attributed to the calculation of recalibrated standards of ossification for the iliac crest apophysis, independent of the imaging modality used. We recommend that the modified 3D-MSCT protocol be referred to for the estimation of age, when post-mortem CT or retrospective clinical MSCT data is available. Our results can be applied to macroscopic skeletal examination if the secondary center is recovered, or referred to in clinical pediatric skeletal surveys using 3D datasets acquired using non-iodising radiation technology i.e. magnetic resonance imaging (MRI) and ultrasonography. Table 6 and Figure 6 demonstrate that the cumulative probit model provides a better fit to the 3D-MSCT data than Risser stages to estimate age, with transition ages between consecutive stages for the 3D-MSCT seven-stage tier around 6-18 months apart. Figure 6 illustrates a more reliable and consistent spread of the age and stage relationship in comparison to Risser, with distinct age delimitation at the extreme ends of each MSCT stage, presented as the smallest probability estimates. Posterior distributions of age for the modified 3D-MSCT methodology suggest that apophyseal ossification (stages I-III) is too variable to be of value for age estimation, yielding low probability estimates (< 50%) of age given MSCT stage (Fig. 9). If a

Queensland female presents with age indicators consistent with Stage 0 (apophysis not present), it can be claimed beyond reasonable doubt that she was 13 years or younger, thus eligible for the *doli capax* presumption. *Doli capax* presumption can be argued for Queensland males if classified into stage IV (commenced union), with a 98.04% probability that he is older than 14 years. The probabilities provided in Figure 9 and credible intervals in Table 7 may be consulted for assessing international ages of criminal responsibility (e.g. minimum age of responsibility: 12 years – Canada; 15 years – Denmark, Norway; 16 years – Japan, Spain) opposed to anthropological standards derived from antiquated skeletal repositories. However, geographically/demographically disperse populations still need to be evaluated to validate the modified 3D-MSCT methodology introduced in this paper and where appropriate construct population-specific standards to increase accuracy of age estimation. Furthermore, for living age estimation efforts of Queensland individuals, we encourage validation of the recalibrated standards on ossification assessment using ultrasonography or MRI.

The oldest probable age for stage III may be consulted for estimating the age of majority under the *Juvenile Justice Act 1992* (QLD) (ss.5, 6 ("child")) and the *Child and Young Persons Act 1989* (VIC) (s.3 ("child")) of 17 years. Using the modified scoring tier, at the age of 17 years there is 79.5% and 86.6% probability that epiphyseal union (of any degree) is evident in Queensland males and females, respectively. For age of majority, which under the *Commonwealth of Australia Constitution Act* (s.109) and remaining Australian states and territories constitutes 18 years, it is probable that 53.1% of individuals exhibit active union (stage V), while 25.3% have commenced union (stage IV). The distribution plots provide evidence that examination of the fusion of the apophysis is more accurate and reliable for age of majority estimation in Queensland and Commonwealth casework than examination of ossification timing (Figs. 4, 6 and 7).

Demographic and Temporality Bias

The results of the modified 3D-MSCT scoring system, which encapsulate the degree of fusion of the apophysis to the ilium in stages IV – VI, are speculative of positive secular change in the maturation of the iliac crest, in comparison to dry bone studies. Australian age standards, segregated for sex, are significantly younger than anthropological standards derived from macroscopic inspection (Table 7) (43-47). It is also important to note that the aforementioned studies utilize antiquated reference samples/collections, featuring the Coimbra Collection (45) with birth years between 1826 – 1922, the Luis Lopes Collection (Lisbon Collection (46)) with the majority of individuals born between 1910 – 1930, and US Korean War Dead born 1951 – 1957 (44). Such repositories are limited to small sample sizes, which are problematic since the true range of biological variation associated with subadult growth cannot be captured, and thus is not representative of or generalizable to the population at large. Nawrocki (48) advised that large samples with even age distributions and equal numbers of both sexes and population groups in each

age interval are required for hypothesis testing; a feat often not attainable in osteological collections or modern donor repositories.

An important consideration pertaining to clinical data acquisition relates to the lack of information associated with the ancestral composition of the population sample. The ancestry of each individual is not recorded upon clinical examination as it is deemed to be medically irrelevant, with the exception of individuals who self-identify as Australian Aboriginal or Torres Strait Islander; collected for health survey purposes. Based on recent Census data (49), the state of Queensland is composed of an amalgamation of ancestral groups: 56.8% of primary resources ascertain European ancestral origins within two generations, followed by 26.3% of Australian (sub-classification of Oceanian), 5.5% Asian ancestry, 3.085% of Australian Indigenous status and 1.1% of African or Middle Eastern origin. For living age estimation efforts of migrants, we recommend that validation studies and subsequent recalibration of age standards be conducted for Asian, Pacific and African population groups, based on global refugee trends (50). In light of an international paucity in age standards for modern children however, the results of this study may be better suited to estimate age in Australian casework, irrespective of national origin of the individual, as opposed to the current, antiquated standards, subject to temporality biases, until similar population-specific studies can be conducted.

Konigsberg (34) raises a valuable point, that there has been a disconnect between studies that focus on osteological scoring methods and those that focus on appropriate statistical methodology for analyzing ordinal data. Comparatively, Cardoso (32) reported that complete fusion was attained between 19 - 21 years of age in males and 18 – 21 years in females; the upper extremity of these ranges slightly older than Australian individuals (19.2 years in males, 20.1 years in females), while complete fusion was documented as early as 17 years in our sample. Coqueugniot and Weaver (31) demonstrated that complete fusion of individuals in the Coimbra collection was attained prior to 24 years in Portuguese males and 26 years in females; considerably delayed by 4.8 years in males and 5.9 years in females relative to the Australian sample; while complete fusion of Australian individuals was attained approximately 3 – 4 years earlier than American individuals, with reference to the McKern and Stewart (44) and Webb and Suchey (43) studies. Similarly, Schaefer (47) reported that fusion commenced at 17 years in Bosnian males who lost their lives during the fall of Srehrenica, in contrast to 13.8 years in Australian males. In comparison to a multi-racial Los Angeles autopsy sample (43), the anterior apophysis appeared approximately 5 years earlier in Australian females, while complete fusion was attained 3 years and 3.8 years earlier in Australian females and males, relative to the US sample. Although cross-study comparisons to the plethora of dry bone anthropological studies are inferred in this manuscript with reference to temporality and demographic biases, they should be interpreted with caution, since our study constitutes the first MSCT examination of iliac crest apophysis and is the only examination to employ statistical modeling approaches that satisfy the recommendations proposed by the Rostock Manifesto.

Conclusions

The current study enhances our understanding of the ontogenic changes of the iliac crest apophysis by overcoming limitations consistent with small sample size and antiquated collections. This manuscript provides a cautionary note on the issues associated with morphological scoring using plain film radiographs, discussing the limitations associated with 2D radiographic appearance and the subsequent delayed aging standards based on the Risser sign. The true ontogenic pattern of ossification is inferred using cross-sectional clinical data acquired from modern subadults, and is reflected in a modified 3D-MSCT scoring-tier, with reported age standards demonstrating a higher discrimination power than the Risser system and higher inter-rater reliability agreement, for utility in age-at-death estimation in forensic contexts, legal age demarcation in criminal proceedings. This investigation constitutes the first to derive probabilistic information for age estimation utilizing a cumulative probit regression model to report complete fusion of the iliac apophysis between 17.3 – 19.2 years in males and 17.1 – 20.1 years in females in Australian individuals. The present study is limited to univariate assessment of the iliac apophysis to assist with constructing the biological profile; no quantitative and systematic means to combine growth data from numerous age indicators is currently available, therefore future research will strive to develop and employ a multi-variable transition analysis model to combine ordinal scores obtained from all available ossification sites of the innominate, including the cranial work conducted by Lottering et al. (26, 31).

Acknowledgements

Gratitude is extended to the Department of Medical Imaging and Nuclear Medicine at the Lady Cilento Children's Hospital, particularly Ms. Debbie Watson, Ms. Kate Barbour and Mr. David Watts; as well as Mr. Michael Saide from the Department of Medical Imaging, Mater Health Services, Brisbane for their tremendous contributions toward the MSCT data acquisition. The authors would like to thank the High Performance Computing and Research Support Group, particularly Mr. Mark Barry for the provision of hardware and OsiriX® licensing utilised in this study. Thanks is extended to Ms. Anne McArdle. (Paediatric Spine Research Group Research Assistant) for retrospective data collection and curation of patient meta-data; this position was supported by funding from a Golden Casket Paediatric and Child Health Grant. We would like to acknowledge Miss Mikaela Reynolds and Mr Gary Bateman (Specialist Spinal Orthotist, GB Orthopaedics, Brisbane) for performing inter-observer grading and Drs Geoffrey Askin and Robert Labrom (Spinal Orthopaedic Surgeons) for Cobb angle measurements and clinical patient data; and Mr. Joseph Smith for his efforts pertaining to graphic design and silhouette representations employed in Figure 3. Ethical approval for this research was granted by The Childrens Health Service District Ethics Committee (HREC/12/QRCH/208), ratified by QUT Research Ethics Unit (Approval No. 1200000716) and approved by The Queensland Government under the Public Health Act (Section 284) 2005 (RD004657).

References

1. Risser JC. The Iliac Apophysis; an Invaluable Sign in the Management of Scoliosis. Clin Orthop. 1958;11:111-9.

2. Schmidt S, Schmeling A, Zwiesigk P, Pfeiffer H, Schulz R. Sonographic Evaluation of Apophyseal Ossification of the Iliac Crest in Forensic Age Diagnostics in Living Individuals. Int J Legal Med. 2011;125(2):271-6.

3. Scoles PV, Salvagno R, Villalba K, Riew D. Relationship of Iliac Crest Maturation to Skeletal and Chronological Age. J Pediatr Orthop. 1988;8:639-44.

4. Wittschieber D, Vieth V, Domnick C, Pfeiffer H, Schmeling A. The Iliac Crest in Forensic Age Diagnostics: Evaluation of the Apophyseal Ossification in Conventional Radiography. Int J Legal Med. 2013;127(2):473-9.

5. Little DG, Sussman MD. The Risser Sign: A Critical Analysis. J Pediatr Orthop. 1994;14(5):569-75.

6. Izumi Y. The Accuracy of Risser Staging. Spine. 1995;20(17):1868-71.

7. Yang J, Bhandarkar A, Suh S, Hong J, Hwang J, Ham C. Evaluation of Accuracy of Plain Radiography in Determining the Risser Stage and Identification of Common Sources of Errors. J Orthop Surg Res. 2014;9(1):1-8.

8. Zaoussis AL, James JI. The Iliac Apophysis and the Evolution of Curves in Scoliosis. J Bone Joint Surg Br. 1958;40(3):442-53.

9. Dhar S, Dangerfield PH, Dorgan JC, Klenerman L. Correlation between Bone Age and Risser's Sign in Adolescent Idiopathic Scoliosis. Spine. 1993;18(1):14-9.

10. Goldberg MS, Poitras B, Mayo NE, Labelle H, Bourassa R, Cloutier R. Observer Variation in Assessing Spinal Curvature and Skeletal Development in Adolescent Idiopathic Scoliosis. Spine. 1988;13(12):1371-7.

11. Hammond KE, Dierckman BD, Burnworth L, Meehan PL, Oswald TS. Inter-Observer and Intra-Observer Reliability of the Risser Sign in a Metropolitan Scoliosis Screening Program. J Pediatr Orthop. 2011;31(8):e80-4.

12. Shuren N, Kasser JR, Emans JB, Rand F. Reevaluation of the Use of the Risser Sign in Idiopathic Scoliosis. Spine. 1992;17(3):359-61.

13. Shapland F, Lewis ME. Brief Communication: A Proposed Osteological Method for the Estimation of Pubertal Stage in Human Skeletal Remains. Am J Phys Anthropol. 2013;151(2):302-10.

14. Heuze Y, Cardoso HF. Testing the Quality of Nonadult Bayesian Dental Age Assessment Methods to Juvenile Skeletal Remains: The Lisbon Collection Children and Secular Trend Effects. Am J Phys Anthropol. 2008;135(3):275-83.

15. Malina R. Secular Trends in Growth, Maturation, and Physical Performance: A Review. Przeglad Antropologiczny-Anthropological Review 2004;67:3-31.

16. Nadler G. Earlier Dental Maturation: Fact or Fiction? Angle Orthod. 1998;68:535–8.

17. Steckel RH, Rose JC, Spencer Larsen C, Walker PL. Skeletal Health in the Western Hemisphere from 4000 B.C. To the Present. Evol Anthr. 2002;11(4):142-55.

18. Stull KE. An Osteometric Evaluation of Age and Sex Differences in the Long Bones of South African Children from the Western Cape. Aracadia: University of Pretoria, 2013.

19. Ulijaszek SJ. Secular Trends in Growth: The Narrowing of Ethnic Differences in Stature. Nutr Bull. 2001;26(1):43-51.

20. Graham CB. Assessment of Bone Maturation-Methods and Pitfalls. Radiol Clin North Am. 1972;10(2):185-202.

21. Lampl M, Johnston FE. Problems in the Aging of Skeletal Juveniles: Perspectives from Maturation Assessments of Living Children. Am J Phys Anthropol. 1996;101(3):345-55.

22. Crowder C, Austin D. Age Ranges of Epiphyseal Fusion in the Distal Tibia and Fibula of Contemporary Males and Females. J Forensic Sci. 2005;50(5):1001-7.

23. Ontell FK, Ivanovic M, Ablin DS, Barlow TW. Bone Age in Children of Diverse Ethnicity. Am J Roentgenol. 1996;167(6):1395-8.

24. Bogin B. Patterns of Human Growth. Cambridge: Cambridge University Press, 1999.

25. Olze A, van Niekerk P, Schulz R, Schmeling A. Studies of the Chronological Course of Wisdom Tooth Eruption in a Black African Population. J Forensic Sci. 2007 Sep;52(5):1161-3.

26. Lottering N, MacGregor DM, Alston CL, Gregory LS. Ontogeny of the Spheno-Occipital Synchondrosis in a Modern Queensland, Australian Population Using Computed Tomography. Am J Phys Anthropol. 2015;157(1):42-57.

27. Australian Human Rights Commission. An Age of Uncertainty: Inquiry into the Treatment of Individuals Suspected of People Smuggling Offences Who Say They Are Children: Australian Parliament. Canberra: Australian Human Right Commission, 2012.

28. Wittschieber D, Schmeling A, Schmidt S, Heindel W, Pfeiffer H, Vieth V. The Risser Sign for Forensic Age Estimation in Living Individuals: A Study of 643 Pelvic Radiographs. Forensic Sci Med Pathol. 2013;9(1):36-43.

29. Lottering N, MacGregor DM, Barry MD, Reynolds MS, Gregory LS. Introducing Standardized Protocols for Anthropological Measurement of Virtual Subadult Crania Using Computed Tomography. J Forensic Rad Imag. 2014;2(1):34-8.

30. Hatch GM, Dedouit F, Christensen AM, Thali MJ, Ruder TD. Radid: A Pictorial Review of Radiologic Identification Using Postmortem Ct. Journal of Forensic Radiology and Imaging. 2014;2(2):52-9.

31. Lottering N, MacGREGOR DM, Watson DA, Alston C, Gregory LS. Introducing Msct Standards for Age Estimation of Modern Australian Subadults Using Postnatal Ossification Timings of Select Cranial and Cervical Sites. J Forensic Sci. 2015.

32. Cicchetti DV. Guidelines, Criteria, and Rules of Thumb for Evaluating Normed and Standardized Assessment Instruments in Psychology. Psychol Assessment. 1994;6(4):284-90.

33. Lottering N, MacGregor DM, Meredith M, Alston CL, Gregory LS. Evaluation of the Suchey–Brooks Method of Age Estimation in an Australian Subpopulation Using Computed Tomography of the Pubic Symphyseal Surface. Am J Phys Anthropol. 2013;150(3):386-99.

34. Konigsberg LW. Multivariate Cumulative Probit for Age Estimation Using Ordinal Categorical Data. Ann Hum Biol. 2015;42(4):368-78.

35. Martin AD, Quinn KM, Park JH. Mcmcpack: Markov Chain Monte Carlo in R. J Stat Softw. 2011;42:1-21.

36. Cowles MK. Accelerating Monte Carlo Markov Chain Convergence for Cumulative-Link Generalized Linear Models. Stat Comp. 1996;6(2):101-11.

37. Scheuer L, Black S. Developmental Juvenile Osteology. 1st Ed ed. New York: Elsevier Academic Press, 2000.

38. Eveleth P, Tanner J. Worldwide Variation in Human Growth. 2nd ed. Cambridge: Cambridge University Press, 1990.

39. Ousley SD. A Radiographic Database for Estimating Biological Parameters in Modern Subadults. Final Technical Report, National Institute of Justice Award Number 2008-Dn-Bx-K152. Available At: Https://Ncjrs.Gov/Pdffiles1/Nij/Grants/242697.Pdf. Erie, PA: Mercyhurst University, 2013.

40. Kotwicki T. Improved Accuracy in Risser Sign Grading with Lateral Spinal Radiography. Eur Spine J. 2008;17(12):1676-85.

41. Jit I, Singh B. A Radiological Study of the Time of Fusion of Certain Epiphyses in Punjabees. J Anat Soc India. 1971;20:457-66.

42. Garn SM, Rohmann CG, Blumenthal T, Silverman FN. Ossification Communalities of the Hand and Other Body Parts: Their Implication to Skeletal Assessment. Am J Phys Anthropol. 1967;27:75-82.

43. Webb PA, Suchey JM. Epiphyseal Union of the Anterior Iliac Crest and Medial Clavicle in a Modern Multiracial Sample of American Males and Females. Am J Phys Anthropol. 1985;68(4):457-66.

44. McKern TW, Stewart TD. Skeletal Age Changes in Young American Males. Analysed from the Standpoint of Age Identification. Technical Report Ep45. Natick, Massachusetts: Quartermaster Research and Development Center, Environmental Protection Research Division, 1957.

45. Coqueugniot H, Weaver TD. Brief Communication: Infracranial Maturation in the Skeletal Collection from Coimbra, Portugal: New Aging Standards for Epiphyseal Union. Am J Phys Anthropol. 2007;134(3):424-37.

46. Cardoso HFV. Epiphyseal Union at the Innominate and Lower Limb in a Modern Portuguese Skeletal Sample, and Age Estimation in Adolescent and Young Adult Male and Female Skeletons. Am J Phys Anthropol. 2008;135(2):161-70.

47. Schaefer MC. A Summary of Epiphyseal Union Timings in Bosnian Males. Int J Osteoarchaeol. 2008;18(5):536-45.

48. Nawrocki SP. The Nature and Sources of Error in the Estimation of Age at Death from the Skeleton. In: Latham KE, Finnegan M, editors. Age Estimation of the Human Skeleton. Springfield: Charles C. Thomas; 2010;79-101.

49. Australian Bureau of Statistics. Australian Demographic Statistics, Table 2: Population Change, Components – States and Territories, 2011. Data Cube: Excel Spreadsheet, Cat.No. 3101.0. . 2011. Available from: http://www.abs.gov.au/AUSSTATS/abs@.nsf/DetailsPage/3101.0Sep 2013?OpenDocument.

50. United Nations High Commissioner for Refugees. Global Trends 2012. Geneva: UNHCR, 2013.

Additional information and reprint requests:

Nicolene Lottering, Ph.D

Discipline of Anatomy and Pathology

School of Medicine, Frome Road, The University of Adelaide

Adelaide, SA, Australia 5005

Email: nicolene.lottering@adelaide.edu.au

TABLES

TABLE 1 – Summary of research studies providing sample demographics and age ranges for Apophyseal Union (fusion) of the Iliac Crest

Author	Year	Assessment	Sex	Sample Size	Ages	Population	Years of Birth	Stages	Unfused[1]	Fusing	Fused[2]
McKern & Stewart	1957	Dry Bone	Male	266	17-25	US Korean War Dead (United States)	1951 – 1957	5	≤ 20	17-23	≥ 18
Jit & Singh	1971	Radiographic	Male	517	11-25	Indian	N/A	5	≤ 19	16-20	≥ 17
			Female	402					≤ 20	15-20	≥ 17
Webb & Suchey	1985	Dry Bone	Male	185	11-40	United States	N/A	4	≤ 19	15-23	≥ 17
			Female	68					≤ 15	14-23	≥ 17
Coqueugnoit &Weaver	2007	Dry Bone	Male	68	7-29	Coimbra Collection	1826 – 1922	3	≤ 20	16-24	≥ 20
			Female	69		(Portuguese)			≤ 19	17-26	≥ 22
Cardoso	2008	Dry Bone	Male	49	9-25	Lisbon Collection	1910 – 1930	3	≤ 18	16-21	≥ 19
			Female	57		(Portuguese)			≤ 16	15-21	≥ 18
Schaefer	2008	Dry Bone	Male	256	14-30	Bosnian	N/A	3	N/A	?-18	≥ 16

[1]Unfused age refers to the oldest probable age, at which the apophysis is present, but no osseous fusion to the ilium is evident; [2]Fused age refers to the youngest age at which complete fusion of the apophysis to the ilium is documented. NOTE: all ages represented as years post-partum; '?' refers to truncated age range, therefore youngest probable age cannot be attained. Stage classifications are based on summary statistics published in each study.

TABLE 2 – MSCT Modified Scoring Criteria for the Stages of Maturation of the Iliac Crest

Stages	Description
0	No apophysis present
I	Anterior and/or posterior apophyseal centers have appeared. However, the combined length is approximately half (50%) or less than the length of the superior border of the ilium.
II	The lengthwise measurement of the anterior and posterior apophyseal centers is greater than 50% of the iliac crest. *Skip ossification* of the posterior superior iliac crest is evident, visualised as a distinct gap greater than 1cm between the adjacent apophyseal centers.
III	Combined lengthwise apophyseal measurement is equal to the length of the curvilinear superior border of the ala of the ilium. The apophyseal centers may be partially or completely united, posterior to the most superior point of the mid-crest. In some instances a small interruption, measuring less than 1cm, between the anterior and posterior apophyseal centers may be visible. *The cartilage between the apophysis and ala of ilium has not ossified*.*
IV	*Commenced Fusion:* Apophyseal fusion to the ala of the ilium has commenced on the anterolateral surfaces of the iliac crest with the apophyseal cartilage ossified less than 50% of its maximum length. The apophysis may not extend to the complete width of the superior border of the ilium.
V	*Active Fusion:* Apophyseal fusion to the ala of the ilium is greater than 50%, typically with sporadic disruption of the radiopaque lamellar bone border, in the regions of the iliac tubercle (antero-lateral flaring) and/or superior to the iliac tuberosity.
VI	*Complete Fusion:* Complete ossification of the apophyseal cartilage; complete osseous fusion of the iliac apophysis with the ilium with either remnant of a sclerotic margin or no remaining vestige.

*Assessment recommended using a multi-planar reformatted model only.

TABLE 3 – Bayesian estimates of age-at-transition (± standard error of the mean, SEM) and standard deviation (SD) from the cumulative probit model for ossification status of the iliac crest apophysis based on the Risser Sign.

Transition	Queensland Males		Queensland Females		
Stage	Estimate (± SEM)	SD	Estimate (± SEM)	SD	*t*-statistic
0-1	14.17 ± 0.11*	0.96	12.89 ± 0.10	1.25	8.61
1-2	14.55 ± 0.10*		13.39 ± 0.09		8.62
2-3	14.88 ± 0.09*		13.83 ± 0.09		8.25
3-4	15.36 ± 0.09*		14.44 ± 0.09		7.23
4-5	16.38 ± 0.11*		15.77 ± 0.10		4.10

Age estimate represented in years post-partum. Degrees of Freedom = ∞. *Statistical significance at $P \leq 0.01$ level.

TABLE 4 – Posterior Density Estimates, including the Posterior mean and credible intervals (CI) in years post-partum, for ossification status of the iliac crest apophysis using the Risser Sign, in Queensland males and females. NOTE: The oldest and youngest probable ages for the first and last stages, were calculated using one-tailed probabilities.

	Stage 0	**Stage 1**	**Stage 2**	**Stage 3**	**Stage 4**	**Stage 5**
Males						
Mean	6.11	13.35	13.71	14.12	14.87	22.16
95%	≤ 13.23	11.42-15.27	11.77-15.62	12.16-16.06	12.87-16.87	≥ 15.28
90%	≤ 12.64	11.74-14.97	12.09-15.32	12.49-15.74	13.20-16.54	≥ 15.88
75%	≤ 11.42	12.22-14.47	12.58-14.84	12.98-15.25	13.70-16.04	≥ 17.08
68%	≤ 10.91	12.39-14.32	12.74-14.67	13.14-15.10	13.85-15.88	≥ 17.56
Females						
Mean	5.51	12.15	12.59	13.12	14.10	21.83
95%	≤ 12.31	9.65-14.64	10.11-15.09	10.65-15.62	11.54-16.70	≥ 14.43
90%	≤ 11.64	10.04-14.22	10.50-14.68	11.05-15.22	11.95-16.27	≥ 15.14
75%	≤ 10.36	10.69-13.61	11.13-14.06	11.67-14.57	12.60-15.61	≥ 16.50
68%	≤ 9.87	10.89-13.41	11.32-13.86	11.87-14.38	12.79-15.41	≥ 17.04

TABLE 5 – Probability of being at a given state of ossification using the Risser Scoring System at Commonwealth legal demarcation ages of 14 years and 18 years for Queensland Males and Females.

Risser Stage	**14 Years Old**		**18 Years Old**	
	Male	Female	Male	Female
0	56.95 (48.47-65.98)	18.92 (15.36-22.79)	0.01 (0.00-0.02)	0.00 (0.00-0.01)
1	14.57 (10.87-18.56)	12.44 (9.45-15.94)	0.02 (0.00-0.06)	0.01 (0.00-0.03)
2	10.44 (7.35-13.75)	13.12 (10.03-16.71)	0.05 (0.01-0.16)	0.03 (0.01-0.09)
3	9.95 (6.97-13.14)	19.20 (15.02-23.73)	0.27 (0.06-0.69)	0.19 (0.06-0.41)
4	7.36 (4.64-10.84)	28.34 (24.15-32.70)	4.48 (1.75-8.39)	3.57 (1.84-5.84)
5	0.72 (0.30-1.34)	7.98 (5.79-10.39)	95.17 (90.74-98.15)	96.19 (93.67-98.08)

Probability statistics, transformed as a percentage, are expressed as the mean (95% credible interval).

TABLE 6 – Bayesian estimates of age-at-transition (± standard error of the mean, SEM) and standard deviation (SD) from the cumulative probit on transition analysis for ossification status of the iliac crest apophysis using a modified 3D-MSCT seven-stage scoring-tier for Queensland individuals.

Transition	**Queensland Males**		**Queensland Females**		
Stage	Estimate (± SEM)	SD	Estimate (± SEM)	SD	*t*-statistic
0-I	13.81 ± 0.15*	0.95	12.20 ± 0.22	1.31	6.05
I-II	14.91 ± 0.13*		13.73 ± 0.19		5.13
II-III	15.75 ± 0.13*		14.90 ± 0.17		3.97
III-IV	16.21 ± 0.13*		15.53 ± 0.17		3.17
IV-V	17.46 ± 0.12		17.25 ± 0.15		1.09
V-VI	18.86 ± 0.13		19.20 ± 0.17		1.59

Age estimate represented in years post-partum. Degrees of Freedom = ∞.

*Statistical significance at $P \leq 0.01$ level.

TABLE 7 – Posterior Density Estimates, including the Posterior mean and credible intervals (CI), for ossification status of the Iliac Crest apophysis in Queensland individuals using the new 3D-MSCT seven-stage scoring tier. NOTE: The oldest and youngest probable ages for the first and last stages, were calculated using one-tailed probabilities.

	Stage 0	**Stage I**	**Stage II**	**Stage III**	**Stage IV**	**Stage V**	**Stage VI**
Males							
Mean	8.96	13.36	14.34	14.99	15.84	17.17	20.86
95%	≤ 13.27	11.35-15.34	12.40-16.29	13.05-16.89	13.82-17.85	15.11-19.22	≥ 17.26
90%	≤ 12.79	11.68-15.03	12.71-15.99	13.36-16.59	14.15-17.52	15.44-18.89	≥ 17.70
75%	≤ 11.92	12.19-14.52	13.20-15.48	13.85-16.11	14.65-17.02	15.96-18.37	≥ 18.47
68%	≤ 11.61	12.35-14.36	13.35-15.32	14.01-15.95	14.81-16.86	16.13-18.20	≥ 18.75
Females							
Mean	8.24	11.96	13.31	14.22	15.38	17.23	20.95
95%	≤ 12.28	9.18-14.72	10.60-16.01	11.61-16.84	12.62-18.15	14.40-20.07	≥ 17.07
90%	≤ 11.72	9.62-14.28	11.04-15.56	12.03-16.44	13.06-17.71	14.86-19.60	≥ 17.62
75%	≤ 10.76	10.33-13.59	11.74-14.89	12.68-15.77	13.75-17.01	15.57-18.88	≥ 18.55
68%	≤ 10.44	10.56-13.37	11.96-14.67	12.88-15.56	13.97-16.79	15.80-18.65	≥ 18.87

TABLE 8 – Test of Posterior Density Functions on an independent sample of Queensland females (n = 20). Grey shading represents incorrect age classification using respective credible intervals (CI). Error quantified using bias and inaccuracy measures, where estimated age is the posterior mean for each sample; average statistics provided in the last row.

Age	Score	Posterior Mean	Predicted 68% CI	Predicted 75% CI	Predicted 90% CI	Predicted 95% CI	Bias
11.5	0	8.2	≤ 10.4	≤ 10.7	≤ 11.7	≤ 12.3	-1.1
12.3	1	11.9	10.5 - 13.4	10.3 - 13.6	9.6 - 14.3	9.3 - 14.7	-0.3
12.5	4	15.4	13.9 - 16.8	13.7 - 17.0	13.1 - 17.7	12.6 - 18.1	2.9
14.1	1	11.9	10.5 - 13.4	10.3 - 13.6	9.6 - 14.3	9.3 - 14.7	-2.1
15.7	2	13.3	11.9 - 14.7	11.7 - 14.9	11.0 - 15.5	10.6 - 16.0	-2.4
16.1	4	15.4	13.9 - 16.8	13.7 - 17.0	13.1 - 17.7	12.6 - 18.1	-0.7
16.2	2	13.3	11.9 - 14.7	11.7 - 14.9	11.0 - 15.5	10.6 - 16.0	-2.9
16.5	4	15.4	13.9 - 16.8	13.7 - 17.0	13.1 - 17.7	12.6 - 18.1	-1.1
16.7	1	11.9	10.5 - 13.4	10.3 - 13.6	9.6 - 14.3	9.3 - 14.7	-4.7
16.9	4	15.4	13.9 - 16.8	13.7 - 17.0	13.1 - 17.7	12.6 - 18.1	-1.4
17.1	4	15.4	13.9 - 16.8	13.7 - 17.0	13.1 - 17.7	12.6 - 18.1	-1.7
17.9	5	17.2	15.8 - 18.7	15.6 - 18.9	14.9 - 19.6	14.4 - 20.1	-0.7
18.4	6	20.9	≥ 18.9	≥ 18.5	≥ 17.6	≥ 17.1	2.5
18.5	5	17.2	15.8 - 18.7	15.6 - 18.9	14.9 - 19.6	14.4 - 20.1	-1.3
18.9	5	17.2	15.8 - 18.7	15.6 - 18.9	14.9 - 19.6	14.4 - 20.1	-1.7
19.1	5	17.2	15.8 - 18.7	15.6 - 18.9	14.9 - 19.6	14.4 - 20.1	-1.9
19.2	5	17.2	15.8 - 18.7	15.6 - 18.9	14.9 - 19.6	14.4 - 20.1	-1.9
19.3	5	17.2	15.8 - 18.7	15.6 - 18.9	14.9 - 19.6	14.4 - 20.1	-2.1
19.3	5	17.2	15.8 - 18.7	15.6 - 18.9	14.9 - 19.6	14.4 - 20.1	-2.1
19.8	5	17.2	15.8 - 18.7	15.6 - 18.9	14.9 - 19.6	14.4 - 20.1	-2.6
				Σ Inaccuracy	**2.01 ± 0.96**	**Σ Bias**	**-1.47 ± 1.65**

TABLE 9 – Probability (%) estimates of being at a given state of ossification using the new 3D-MSCT methodology (Table 2) at Commonwealth legal demarcation ages 14 and 18 years for males and females.

MSCT Stage	**14 Years Old**		**18 Years Old**	
	Male	Female	Male	Female
0	42.2 (31.7-54.0)	8.8 (5.3-13.5)	0.0 (0.0-0.1)	0.0 (0.0-0.0)
I	40.7 (31.1-49.5)	33.2 (23.7-43.0)	0.1 (0.0-2.7)	0.1 (0.0-0.2)
II	13.7 (8.2-20.7)	33.1 (24.5-42.4)	0.9 (0.3-12.8)	0.9 (0.3-1.9)
III	2.3 (0.9-4.3)	12.2 (7.5-18.5)	2.1 (0.8-16.6)	2.1 (0.9-4.3)
IV	1.1 (0.4-2.2)	11.7 (7.1-18.0)	25.3 (17.8-57.1)	25.4 (18.2-33.0)
V	0.0 (0.0-0.1)	0.7 (0.3-1.5)	53.1 (45.2-37.7)	53.1 (45.1-60.9)
VI	0.0 (0.0-0.0)	0.0 (0.0-0.0)	18.4 (12.4-4.4)	18.3 (12.7-24.7)

Probability statistics, transformed as a percentage, are expressed as the mean (95% credible interval).